Electronic Supplementary Information (ESI†)

A regioisomeric phenanthroquinoxaline-based small molecular defect passivation layer for enhanced efficiency in stable perovskite solar cells

*Buddhadeb Mondal,[aŦ] Yash Taneja,[bŦ] Chitrak Ghosh,[a] Ranbir Singh, [*b] Suman Kalyan Samanata[*a]*

[a] Department of Chemistry, Indian Institute of Technology Kharagpur, Kharagpur 721302, India; Email: *sksamanta@chem.iitkgp.ac.in*

[b] School of Mechanical and Materials Engineering (SMME), Indian Institute of Technology Mandi (IIT Mandi), Kamand, Mandi, 175005, Himachal Pradesh, India; Email: *ranbir@iitmandi.ac.in*

Ŧ These authors contributed equally to this work.

1. Synthesis:

Syntheses of the key intermediate compounds **1**, **2**, and **3** were reported in previous literature. The detailed synthesis procedure and schematic of the passivators, **PNQP,** and **PNQO,** are given below.[1-3]

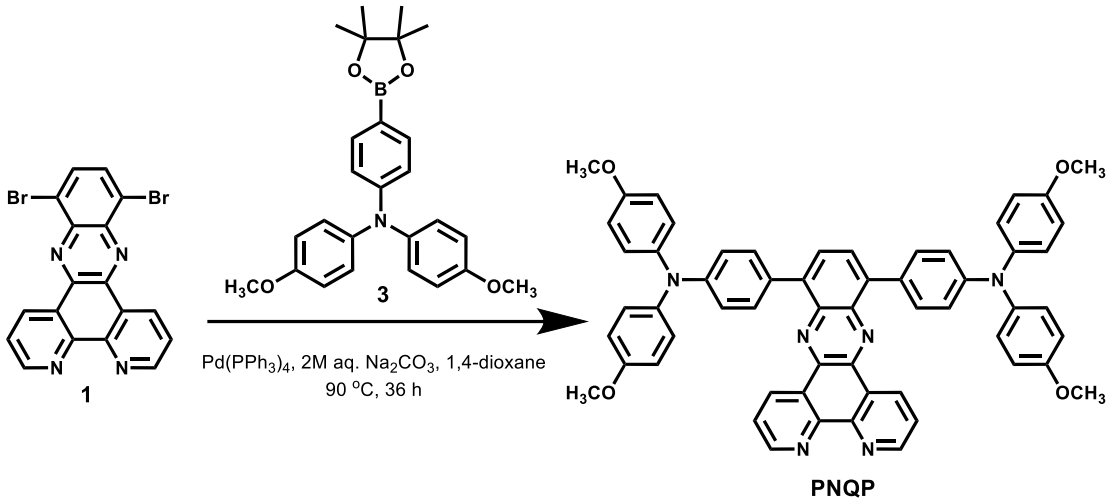

Scheme S1. Synthetic scheme for compound **PNQP**.

Synthesis of PNQP: A mixture of compound **1** (200 mg, 0.45 mmol), 4-methoxy-N-(4-methoxyphenyl)-N-(4-(4,4,5,5-tetramethyl-1,3,2-dioxaborolan-2-yl)phenyl)aniline (444 mg, 0.99 mmol), and $Pd(PPh_3)_4$ (20 mg, 0.02 mmol) was dissolved in 15 mL 1,4-dioxane under an argon atmosphere. Aqueous sodium carbonate solution (2 M, 5 mL) was added to the reaction mixture, which was stirred at 90 °C for 36 h. After being cooled to room temperature, the reaction mixture was extracted with dichloromethane and water (3 × 15 mL). The combined organic layers were washed with water and dried over anhydrous Na_2SO_4. After removing the solvent, the crude product was purified by column chromatography on neutral silica gel with petroleum ether/DCM (1/2, v/v) as eluent to obtain **PNQP** (302 mg, 75% yield) as a purple solid. ^{1}H NMR (400 MHz, Chloroform-d) δ 9.37 (dd, *J* = 8.1, 1.7 Hz, 2H), 9.23 (dd, *J* = 4.4, 1.7 Hz, 2H), 8.00 (s, 2H), 7.80 (d, *J* = 8.1 Hz, 4H), 7.72 (dd, *J* = 8.1, 4.4 Hz, 2H), 7.24 – 7.21 (m, 8H), 7.16 (d, *J* = 8.1 Hz, 4H), 6.95 – 6.87 (m, 8H), 3.84 (s, 12H). ^{13}C NMR (125 MHz, Chloroform-d) δ 156.27, 152.45, 148.66, 140.98, 140.74, 139.81, 138.99, 134.15, 131.84, 130.18, 128.07, 127.12, 124.33, 119.65, 114.96, 55.68.

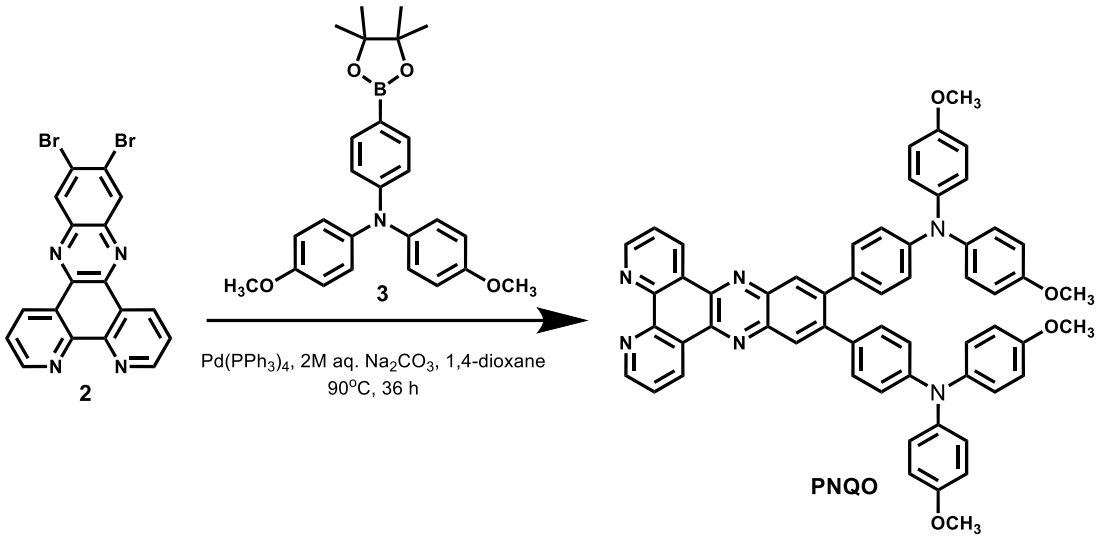

Scheme S2. Synthetic scheme for compound **PNQO**.

Synthesis of PNQO: A mixture of compound **2** (200 mg, 0.45 mmol), 4-methoxy-N-(4-methoxyphenyl)-N-(4-(4,4,5,5-tetramethyl-1,3,2-dioxaborolan-2-yl)phenyl)aniline (444 mg, 0.99 mmol), and $Pd(PPh_3)_4$ (20 mg, 0.02 mmol) was dissolved in 15 mL 1,4-dioxane under an argon atmosphere. Aqueous sodium carbonate solution (2 M, 5 mL) was added to the reaction mixture, which was stirred at 90 °C for 36 h. After being cooled to room temperature, the reaction mixture was extracted with dichloromethane and water (3 × 15 mL). The combined organic layers were washed with water and dried over anhydrous Na_2SO_4. After removing the solvent, the crude product was purified by column chromatography on neutral silica gel with petroleum ether/DCM (1/3, v/v) as eluent to obtain **PNQO** (326 mg, 81% yield) as a brown solid. ^{1}H NMR (400 MHz, $CDCl_3$) δ 9.59 (dd, J = 8.1, 1.7 Hz, 2H), 9.25 (dd, J = 4.4, 1.7 Hz, 2H), 8.29 (s, 2H), 7.76 (dd, J = 8.1, 4.4 Hz, 2H), 7.14 (dt, J = 5.1, 2.7 Hz, 4H), 7.12 – 7.08 (m, 8H), 6.92 – 6.84 (m, 12H), 3.81 (s, 12H).^{13}C NMR (125 MHz, Chloroform-d) δ 156.69, 152.96, 148.91, 148.76, 145.23, 142.55, 141.34, 134.28, 132.73, 131.25, 128.07, 127.43, 124.72, 120.17, 115.41, 56.15.

2. Characterization

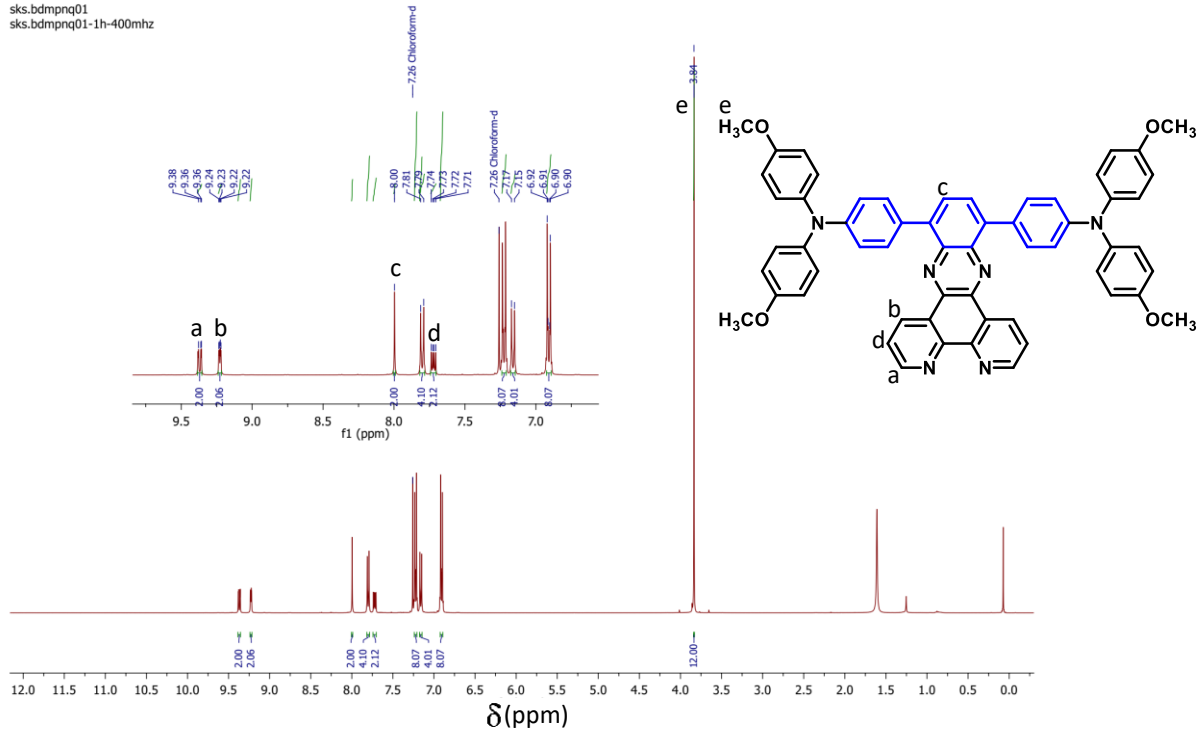

^{1}H NMR of PNQO (400 MHz) with $CDCl_3$ solvent at 298K

Fig. S1. ^{1}H NMR spectrum of **PNQP** in $CDCl_3$ at 25 °C.

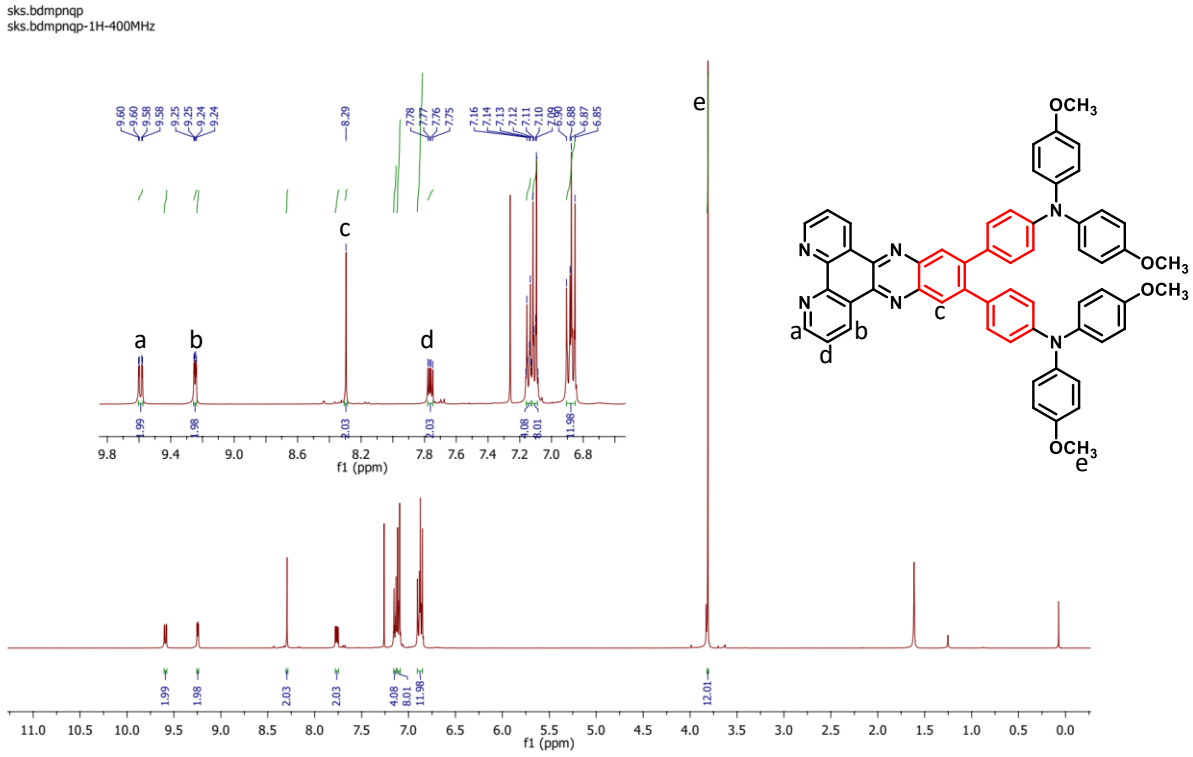

Fig. S2. ^{1}H NMR spectrum of **PNQO** in $CDCl_3$ at 25 °C.

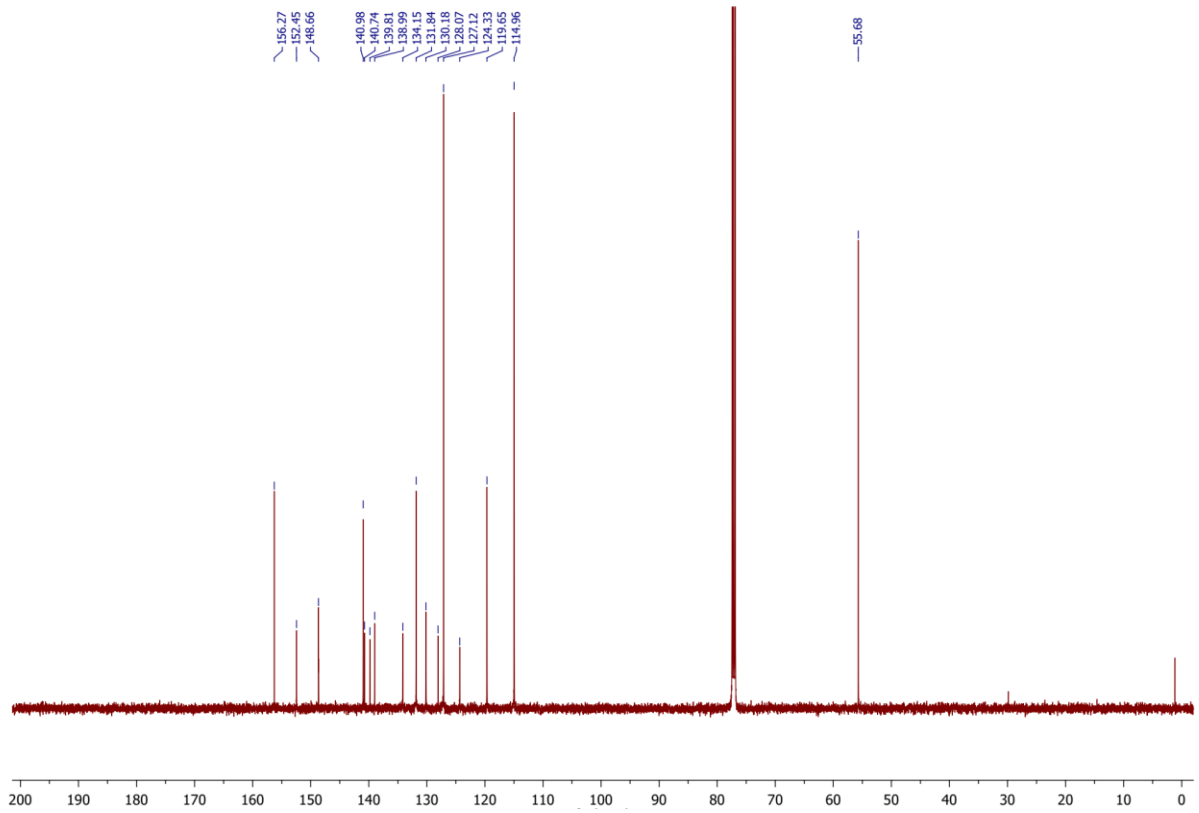

Fig. S3. ^{13}C NMR spectrum of **PNQP** in $CDCl_3$ at 25 °C.

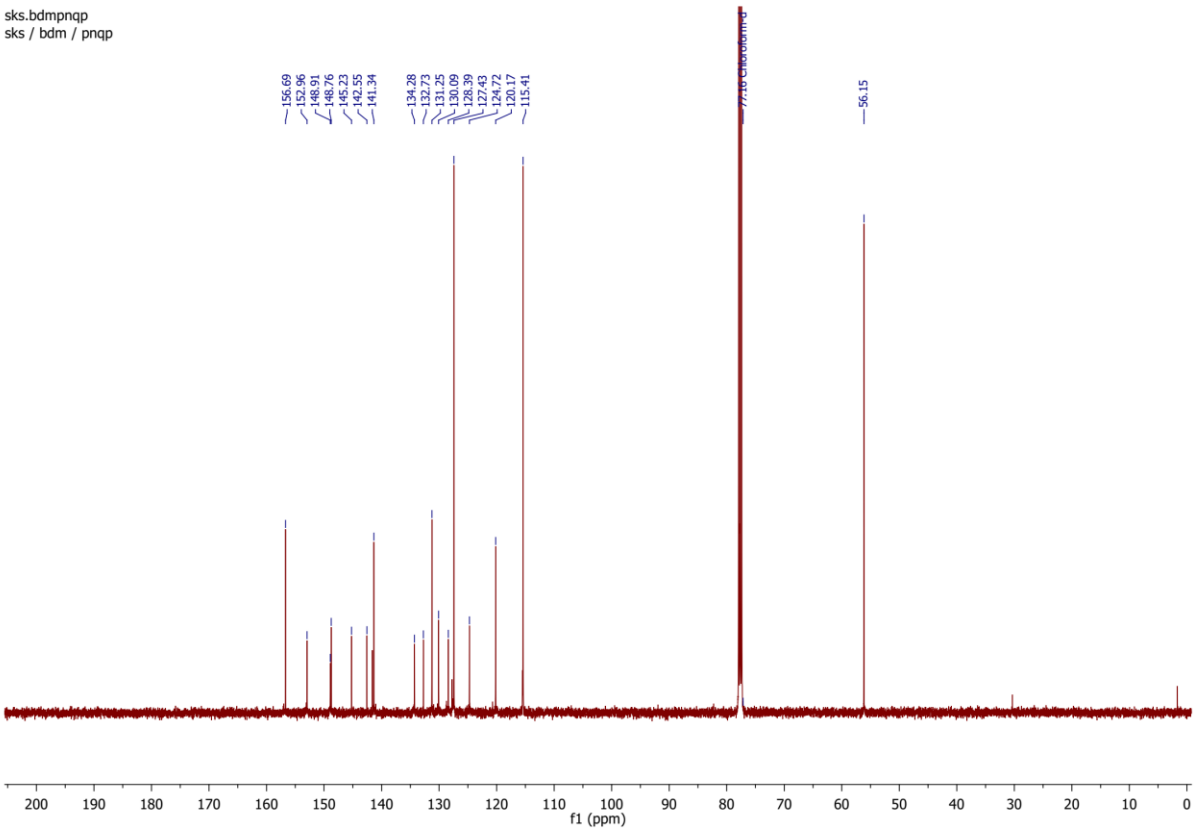

Fig. S4. ^{13}C NMR spectrum of **PNQO** in $CDCl_3$ at 25 °C.

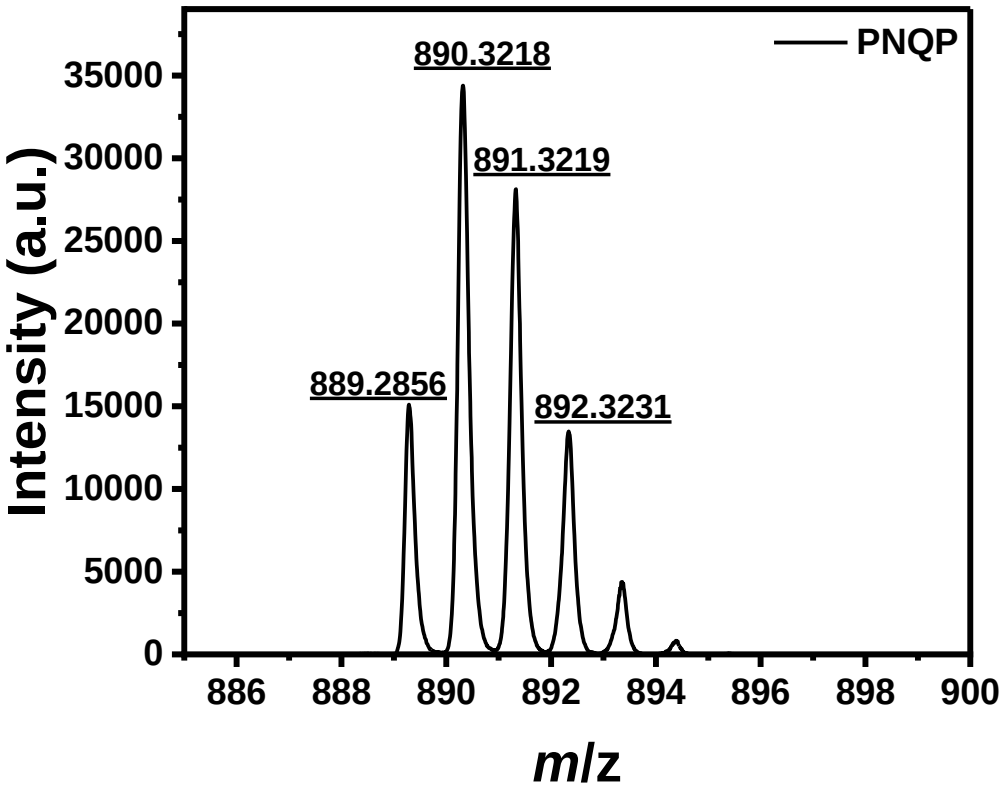

Fig. S5. MALDI-TOF of compound **PNQP.**

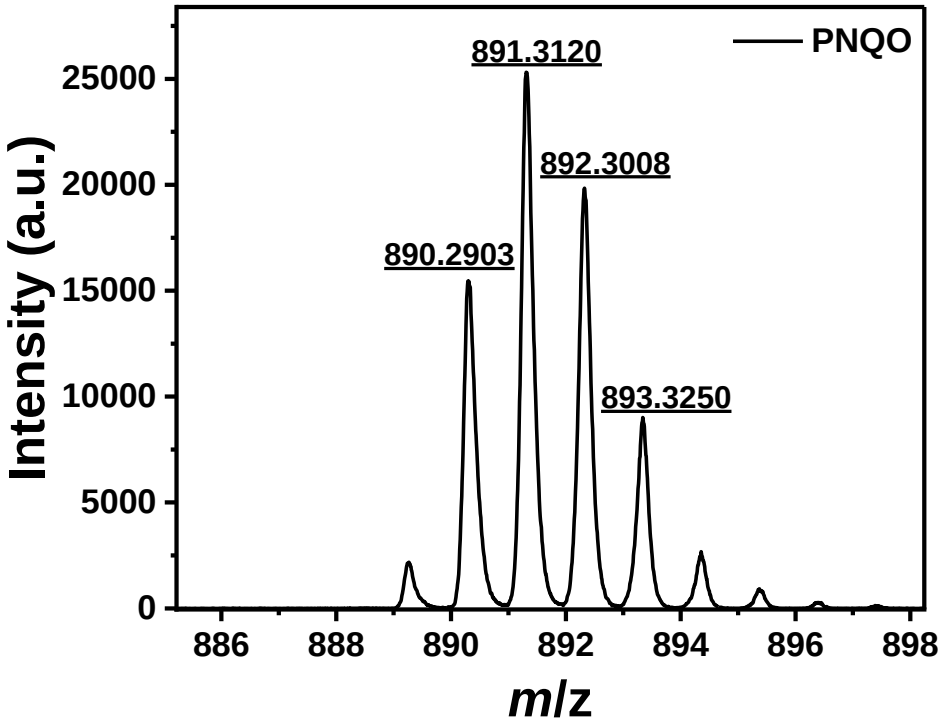

Fig. S6. MALDI-TOF of compound **PNQO.**

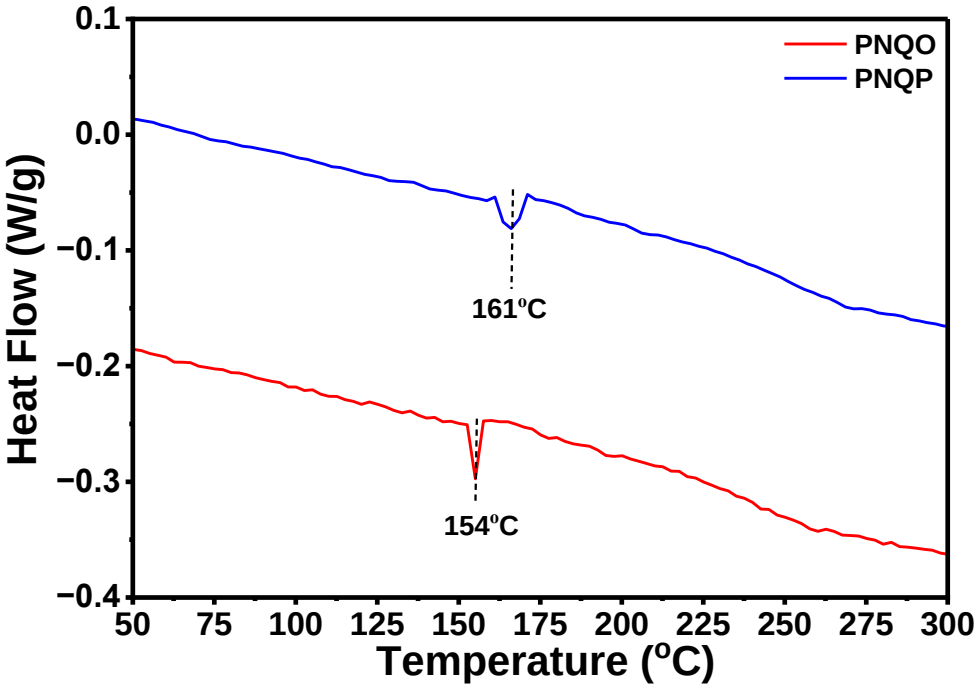

Fig. S7. DSC curves recorded for the **PNQP** and **PNQO** under nitrogen at a heating rate of 10 °C min^{-1} (second cycle).

3. Computational analysis

The geometry of all the model compounds was optimized with the Gauss view 6.0 package and GAUSSIAN 16 software using the DFT/B3LYP/631G basis set.[4] The TD-DFT calculations for the excited states were conducted using the CAM-B3LYP functional, comprising long-range corrections with the same basis set. For TDDFT calculations, Grimme's dispersion model D3[5] was employed to consider the non-covalent interaction. To ensure consistency with the experimental conditions, we considered a self-consistent reaction field (SCRF) model utilizing the SMD[6] approach. The experimental solvent consisted of $CHCl_3$. Natural bonding orbital analysis (NBO) was conducted using the built-in NBO 3.1 module within Gaussian 16. Hole reorganization energy (λ) can be calculated by using the formula

$$\lambda_h = (E^+_{NG} - E^0_{NG}) + (E^0_{CG} - E^+_{CG})$$

Where E^0_{NG} and E^+_{CG} are energies of neutral and cation molecules at the ground and cationic state, respectively. E^0_{CG} and E^+_{NG} are the energies of neutral and cation molecules at cationic and ground states, respectively.

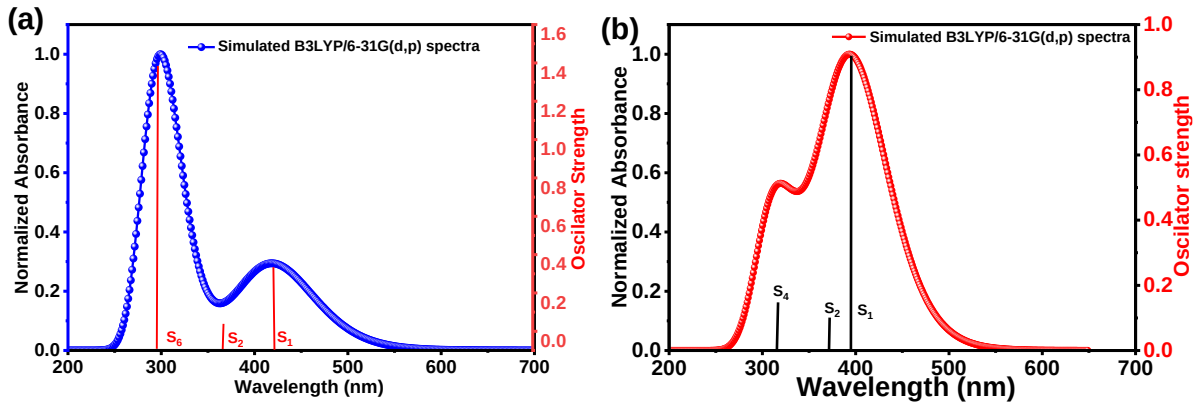

Fig. S8. Simulated absorption spectra of investigated passivators at the TDDFT/B3LYP/6-31G (d,p) level of theory using $CHCl_3$ as a solvent.

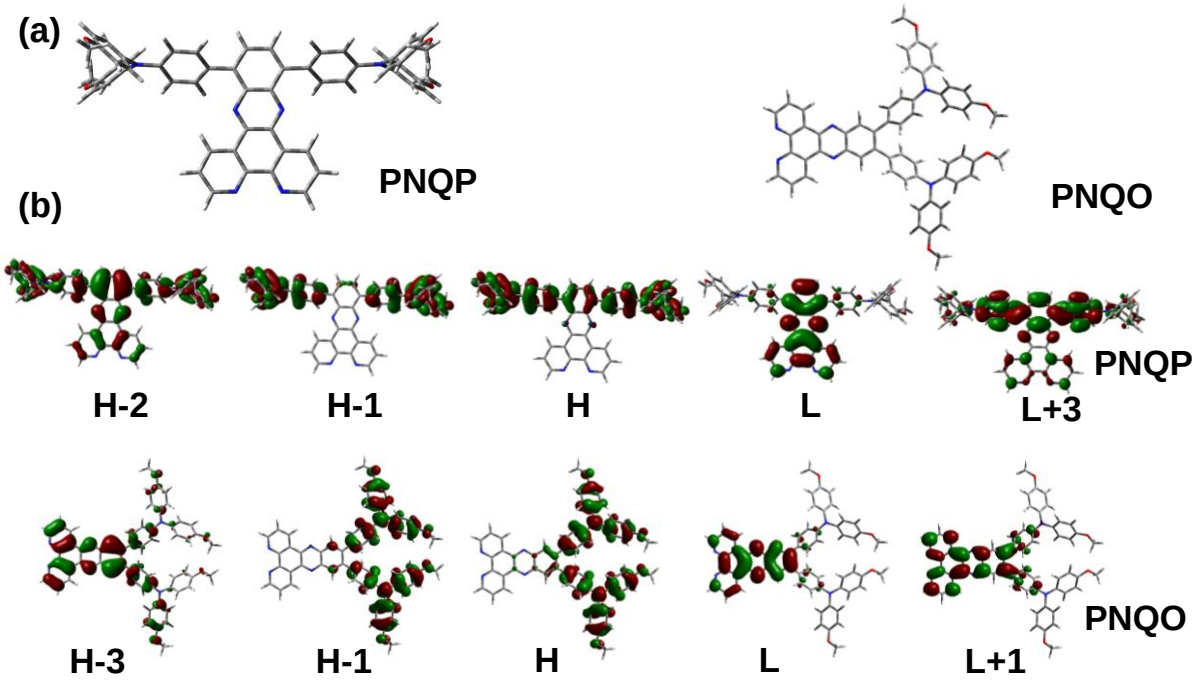

Fig. S9. B3LYP/6-31G(d,p) PCM minimum-energy structures (a) and frontier molecular orbitals (b) calculated for **PNQP** and **PNQO** in $CHCl_3$. H and L stand for HOMO and LUMO, respectively. Atom colour code: C (gray), S (yellow), N (blue), O (red) and H (white).

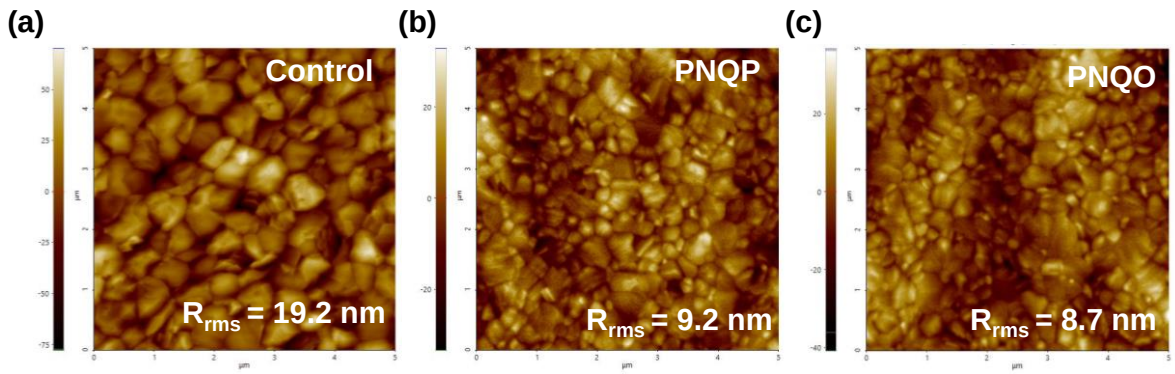

Fig. S10. AFM images of the control perovskite film and the perovskite films modified with PNQP and PNQO.

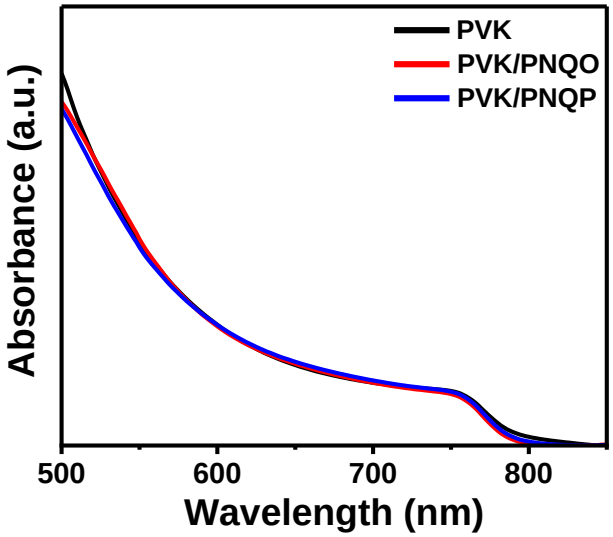

Fig. S11. UV-vis absorption spectra of perovskite films capped with different passivation layers.

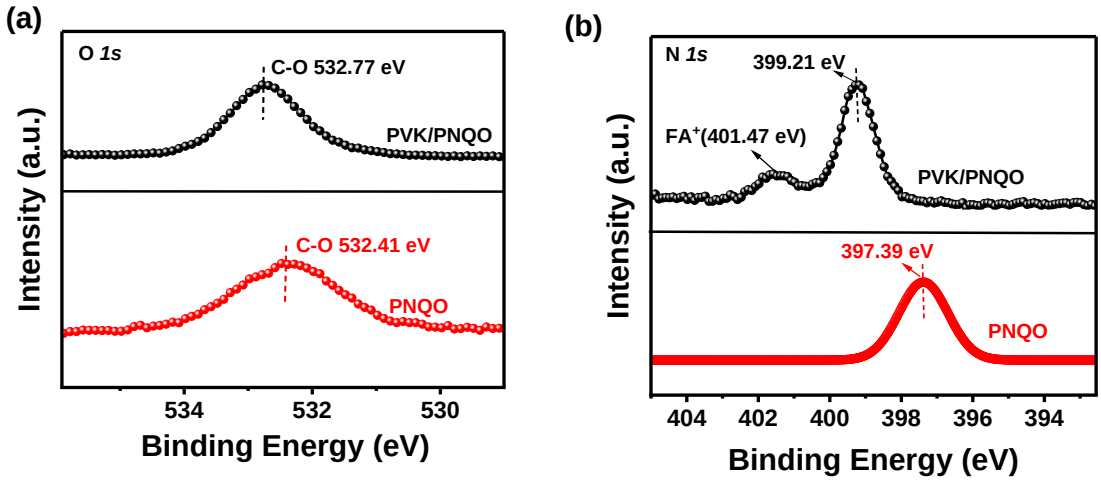

Fig. S12. (a) O 1s, (b) N 1s XPS spectra of pure **PNQO** film and **PNQO**/PVK film.

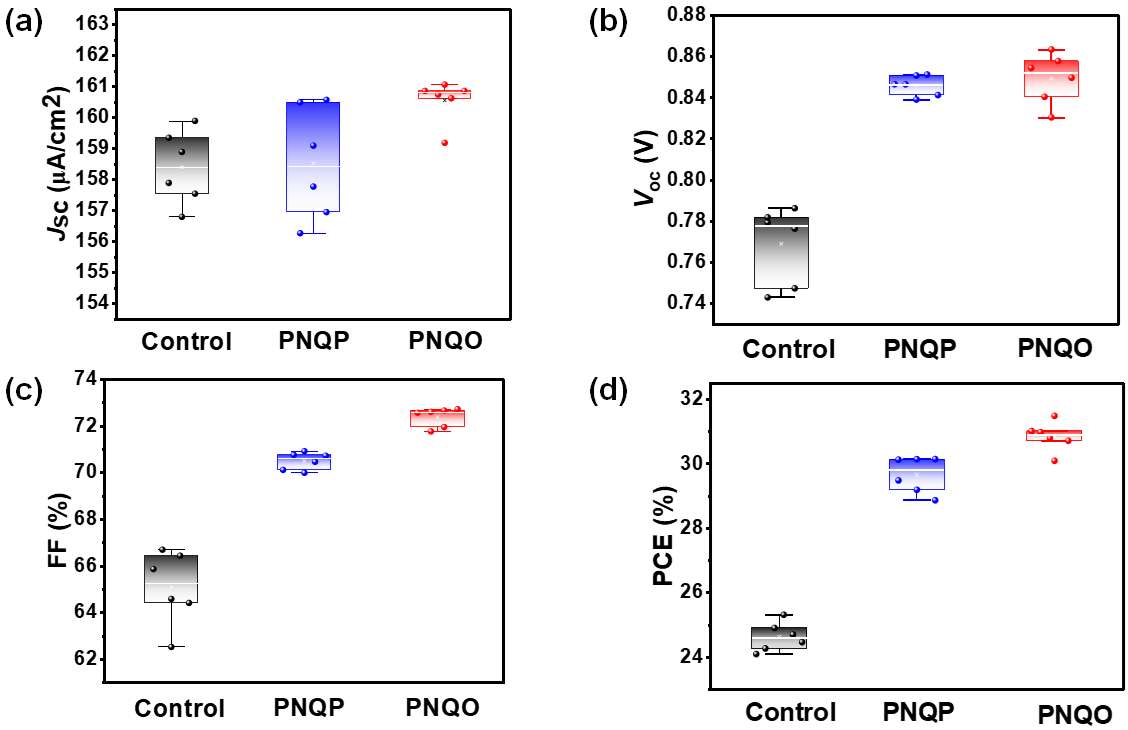

Figure S13. Statistics of the photovoltaic parameter distributions of independent 6 devices based on different passivation layers (indoor condition), (a) current density, (b) open circuit voltage, (c) fill factor, and (d) power conversion efficiency.

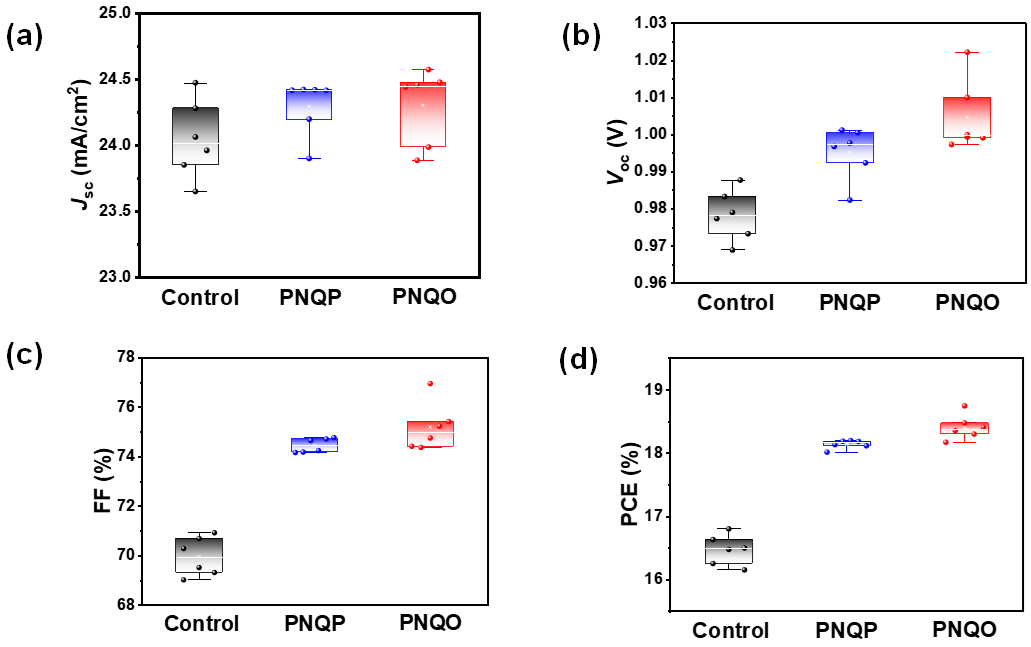

Figure S14. Statistics of the photovoltaic parameter distributions of independent 6 devices based on different passivation layers (outdoor condition), (a) current density, (b) open circuit voltage, (c) fill factor, and (d) power conversion efficiency.

Table S1. TRPL decay lifetime of the perovskite film treated with different interfacial layers.

Compounds	A1 (%)	A2 (%)	τ_1 (ns)	τ_2 (ns)	τ_{avg} (ns)
PVK	81.27	18.73	0.75	45.95	27.12
PNQP treated	87.94	12.06	0.73	15.58	6.11
PNQO treated	90.70	9.30	0.72	15.98	3.47

Table S2. PV Performance of PNQO, PNQP treated devices under AM 1.5G (100 mW cm^{-2})

Samples	J_{sc} (mA/cm^2)	V_{oc} (V)	FF (%)	PCE (%)
Control[a]	24.27	0.97	70.69	**16.64**
	24.01±0.34	0.98±0.01	70.13±1.01	**16.40±0.48**
PNQP treated	24.49	1.01	74.25	**18.36**
	24.20±0.30	0.99±0.015	74.10±0.15	**18.18±0.18**
PNQO treated	24.58	1.02	74.76	**18.74**
	24.20±0.40	1.01±0.01	75.08±1.20	**18.36±0.40**

[a]Doped Spiro-OMeTAD as HTM without a passivation layer

Table S3. EIS parameters of different PSCs

Samples	R_s	R_{ct}
Control	18.84 Ω	3702 Ω
PNQP	17.84 Ω	3391Ω
PNQO	15.67 Ω	3264 Ω

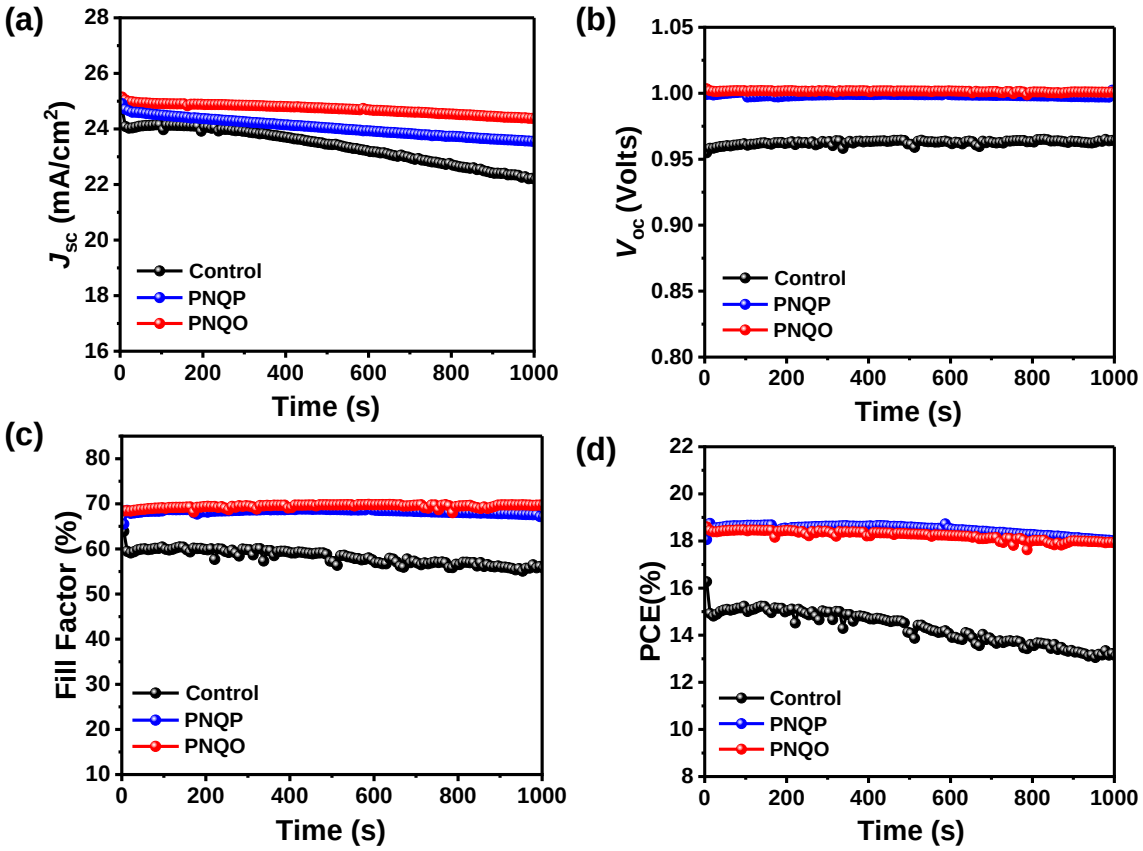

Fig. S15. Light soaking stability data (a) J_{sc}, (b) V_{oc}, (c) FF, (d) PCE of PSCs with and without passivators under AM 1.5 G light illumination.

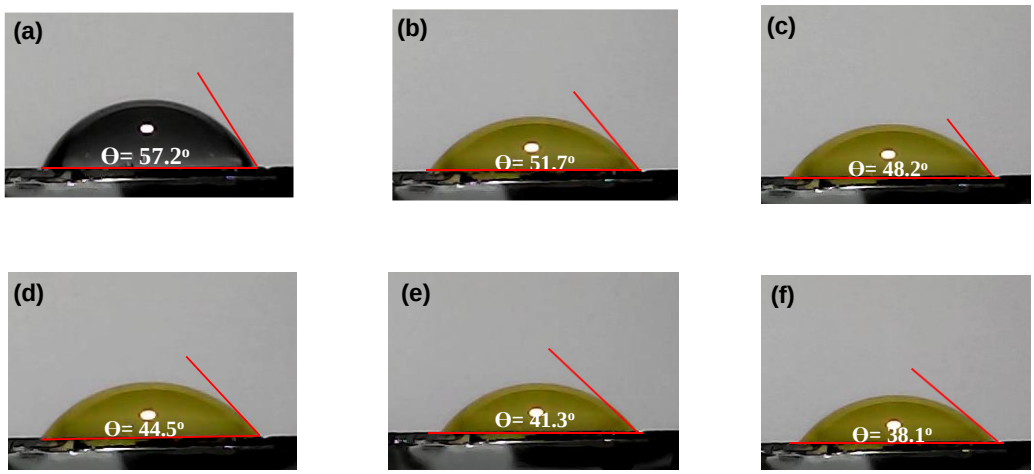

Fig. S16. Water contact angle of bare perovskite at (a) 0 sec, (b) 30 sec, (c) 60 sec, (d) 90 sec, (e) 180 sec, (f) 300 sec.

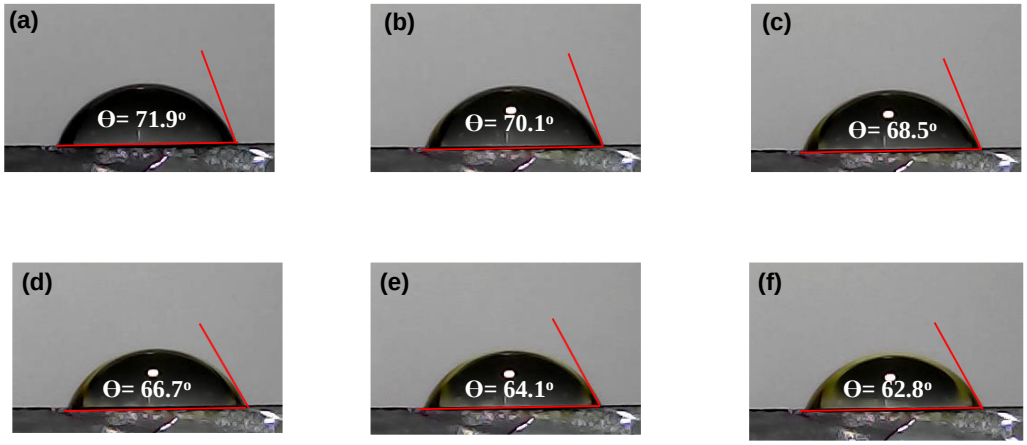

Fig. S17. Water contact angle of **PNQP**-treated perovskite film at (a) 0 sec, (b) 30 sec, (c) 60 sec, (d) 90 sec, (e) 180 sec, (f) 300 sec.

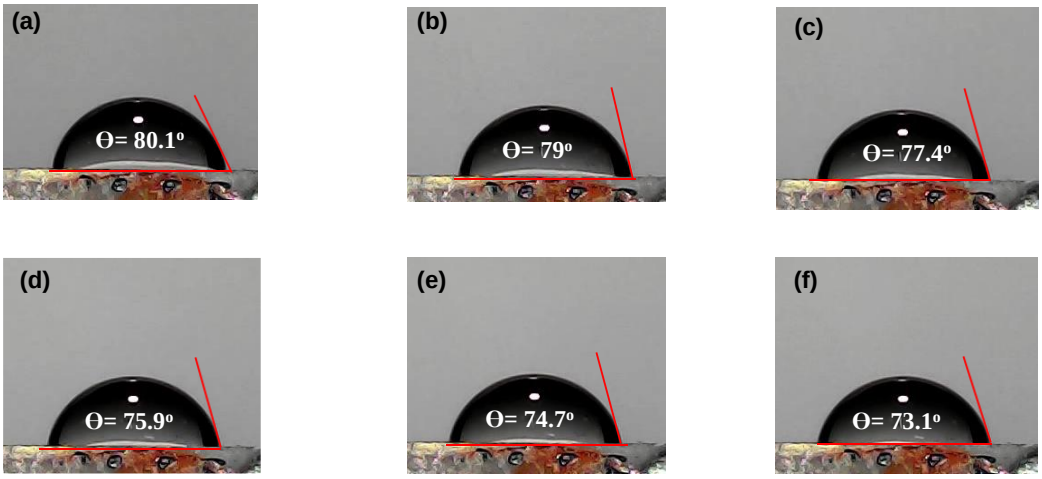

Fig. S18. Water contact angle of **PNQO**-treated perovskite film at (a) 0 sec, (b) 30 sec, (c) 60 sec, (d) 90 sec, (e) 180 sec, (f) 300 sec.

4. References:

1. H.-L. Jia, Z.-J. Peng, S.-S. Li, C.-Y. Huang and M.-Y. Guan, *ACS Appl. Mater. Interfaces*, 2019, **11**, 15845-15852.
2. Y. Zhou, L. Bai, Y.-Y. Gu, L. Tian, H. Yin, Y.-Y. Zhang, H.-W. Zhang, D.-G. Xing and Y.-J. Liu, *Inorg. Chem. Commun.*, 2020, **118**, 108012.
3. B. X. Zhao, C. Yao, K. Gu, T. Liu, Y. Xia and Y.-L. Loo, *Energy Environ. Sci.*, 2020, **13**, 4334-4343.
4. A. D. Becke, *The Journal of Chemical Physics*, 1992, **96**, 2155-2160.
5. S. Grimme, J. Antony, S. Ehrlich and H. Krieg, *J. Chem. Phys.*, 2010, **132**, 154104.
6. A. V. Marenich, C. J. Cramer and D. G. Truhlar, *J. Phys. Chem. B*, 2009, **113**, 6378-6396.